sustainability

MDPI

Article

Investigation of Some Property Changes of Light-Colored Turkish Natural Stones after High-Temperature Treatments

Engin Özdemir

Faculty of Engineering, Inonu University, Malatya 44280, Turkey; ozdemir.engin@inonu.edu.tr; Tel.: +90-422-377-47-32

Abstract: Natural stones are a widely used construction material for both structural and decorative purposes. It is a material used for many floors and cladding due to its special beauty and quite aesthetic appearance. However, natural stones are exposed to different temperatures due to natural, urban or industrial activities and they lose their physico-mechanical properties. It is known that high temperatures and fire cause degradation of construction and building stones. There are many studies investigating the effect of high temperatures on physical and mechanical properties of natural stones, while there are very limited studies on color and gloss. In this study, the changing physical and mechanical properties, color and gloss of different light-colored polished natural stones exposed to room temperature up to 1000 °C in the oven were investigated. For this purpose, natural stones were gradually exposed to 200, 400, 600, 800 and 1000 °C, starting from room temperature. After exposure to different temperatures, water absorption, porosity, Schmidt hammer hardness, point load strength, color and gloss were measured and compared to reference samples (at room temperature). However, all samples were decayed at 1000 °C, changes at this temperature value could not be determined. The results obtained at other temperature values were evaluated separately for each parameter. While the change in physico-mechanical properties of all samples up to 400 °C was limited, a dramatic change was observed with increasing temperature. In all samples, point load strength losses were observed due to an increase in porosity and water absorption. In addition, all samples darkened at 400 °C, while the whiteness value (L*) of samples increased at 800 °C. Gloss values gradually decreased due to the increase in temperature.

Keywords: natural stones; temperature; fire; thermal effect; point load strength; porosity; color; gloss

Citation: Özdemir, E. Investigation of Some Property Changes of Light-Colored Turkish Natural Stones after High-Temperature Treatments. *Sustainability* **2022**, *14*, 10298. https://doi.org/10.3390/su141610298

Academic Editors: Jian Zhou, Mahdi Hasanipanah and Danial Jahed Armaghan

Received: 26 June 2022
Accepted: 15 August 2022
Published: 18 August 2022

1. Introduction

Natural stones are one of the oldest building materials used by humans. Even when people resided in places made of clay and wood, they used natural stones in their various monumental structures. Until the 20th century, natural stones were used instead of bricks in Europe's important and large buildings. There are countless historical monuments made of natural stone in Anatolia, especially during the Ancient Greek, Roman, Byzantine, Seljuk and Ottoman periods. In Seljuk and Ottoman architecture, limestone and tuffs were handled with great skill and decorated the exterior and interior of buildings such as mosques and madrasas. Therefore, Turkey has an important position due to the use of natural stone as a construction and building material [1,2]

Natural stone products, such as marble, travertine, andesite, tuff and granite, are widely used construction materials for both structural and decorative purposes. In particular, they have been used in the construction industry for purposes such as interior–exterior coatings, flooring and landscaping. Natural stones are subject to physical and chemical changes due to different environmental conditions and lose their initial strength properties. While determining the usage areas of natural stones, not only their physico-mechanical properties, but also the environmental factors to which they are exposed, should be determined. Some researchers investigated the effects of environmental conditions, such

as temperature, freeze–thaw, salt crystallization, contact with acid-based solutions and wetting–drying of natural stones. Mutlutürk et al. (2004) developed a model to predict their changes depending on environmental cycles (freezing–thawing and heating–cooling) with an experimental study on 10 different rock types [3]. Yavuz (2011) determined that andesite caused decreases in P-wave velocity, Schmidt hammer hardness and compressive strength, and an increase in porosity and water absorption values, depending on the increase in the number of cycles of thermal shock and freeze–thaw [4]. Fener and Ince (2015) investigated changes in porosity, P-wave velocity, uniaxial compressive strength, point load strength, Bohme abrasion loss and Brazilian tensile strength of Konya–Sille andesite exposed to five F–T cycles [5]. They also evaluated the degree of degradation of structures built with Sille andesite. Ghobadi and Babazadeh (2015) examined changes in weight loss, Vp wave velocity, point load strength and uniaxial compressive strength values, by exposing nine different sandstones from Qazvin region (Western Iran) to accelerated tests (salt crystallization, freeze–thaw, warming–cooling, warming–cooling–wetting) [6]. Gökçe et al. (2016) investigated changes in physico-mechanical (porosity, P-wave velocity, point load strength, uniaxial compressive strength, Bohme abrasion loss and Brazilian tensile strength) properties of Konya–Gödene travertine due to freeze–thaw cycles. They obtained statistical relationships with experimental results obtained in F–T cycles [7]. Bozdag et al. (2016) determined the relationships between weathering and welding degree of pyroclastic rocks in the ancient city of Konya Kilistra by performing accelerated aging tests (freeze–thaw, salt crystallization and wetting–drying). The researchers stated that all three accelerated tests had negative effects on the physico-mechanical properties of rocks, but that F–T and SC were more destructive than WD [8]. Heidari et al. (2017) investigated changes in physico-mechanical properties of samples obtained from Chelmaran quarry after aging tests (freeze–thaw and salt crystallization). They stated that the mechanical strength of the rocks decreased considerably in both cycles [9]. Özşen et al. (2017) researched the effect of salt crystallization on physico-mechanical changes of pyroclastic rock samples collected from six different quarries in Cappadocia. Researchers found strong logarithmic relationships between dry weight loss values and mechanical strength properties [10]. Deng et al. (2018) experimentally investigated combined effects of acid and freeze–thaw cycles on sandstones. The combined effect of acid corrosion and freeze–thaw was found to be more destructive than acid corrosion [11]. Sun and Zhang (2019) researched the effect on the physico-mechanical properties of sandstones exposed to wetting–drying cycles with different saline solutions (0%, 4%, 6% and 8% magnesium sulfate). They stated that samples exposed to salt solution were more affected than pure water [12]. Amirkiyaei et al. (2020) conducted experimental investigations on 22 carbonate building stones (3 limestone, 12 travertine and 7 marble) extracted from different locations in Iran. Based on the data obtained, they developed an empirical equation to determine the Vp wave velocity of stones during freeze–thaw cycles [13]. Guler et al. (2021) investigated changes in physical, mechanical and index properties of six different carbonate rocks by exposing them to thermal cycles. They stated that as the number of T–S and F–T cycles increases, the internal structure of carbonate rocks increases and, as a result, their physico-mechanical properties change significantly [14]. Mardoukhi et al. (2021) determined the effect of test temperature and low temperature thermal cycles on the dynamic tensile strength of rocks in low temperature environments such as Mars. They emphasized that there is an increase in the mechanical strength of granitic rocks due to decreases in temperature, thus this increase should be taken into account in excavation operations [15].

High temperatures are one of main physical agents that cause durability problems of natural stones. Natural stones, which are used as building materials, are exposed to high temperature effects, generally due to fires. These stones deteriorate due to various fires that occur in the natural environment and internal structure of buildings. In the natural environment, fire emerges as a common tool effective in geomorphological and biological change. In such events, temperatures can exceed 1000 °C [16–19]. Fire causes physical and chemical degradation by affecting the material structure. Physical degradation is generally

observed as thermal deformations. Thermal deformations are physical magnitudes that occur within a material under different temperature effects and can generally be seen as thermal expansion or contraction. Many stone buildings have been destroyed as a result of fire damage throughout historical ages [20,21]. Hajpál (2002) stated that the potential impact of fires on buildings can be calculated during the construction of buildings; this data obtained from the buildings affected by fire can be used when constructing new stone buildings, and it is also possible to calculate the risk of such stone buildings. It has been stated that change in the physico-mechanical structure of rocks due to fire reduces the bearing capacity of the building [22]. Tian et al. (2014) experimentally investigated the changes in bulk density and the uniaxial and triaxial compressive strength of claystone exposed to high temperatures from room temperature (23 °C) to 1000 °C at laboratory scale [23]. Ozguven and Ozcelik (2014) investigated the changes in some physico-mechanical properties of eight different natural stones (limestones and marbles) exposed to high temperatures. They stated that there is a decrease in the mechanical strength of natural stones at every stage due to the increase in temperature values from room temperature (23 °C) to 1000 °C [24].

In this study, changes in physico-mechanical properties of five different light-colored natural stones were experimentally investigated by exposing them from room temperature to 800 °C. In particular, non-destructive test methods, such as hardness, porosity, water absorption, Schmidt hammer hardness, color and gloss, were chosen. Thus, the aim is to predict the changes in the physico-mechanical properties of natural stones exposed to fire or high temperatures. In addition, point load strength, which is the most common test method used in the estimation of both the uniaxial compressive and tensile strengths of rocks, was determined. For this purpose, the physico-mechanical changes of natural stones were investigated experimentally by exposing them to different temperatures (23, 200, 400, 600 and 800 °C). The importance of this study is that it contributes to the limited literature on color and gloss changes of natural stones after exposure to high temperatures. In particular, in the restoration of historical buildings after fires, in addition to physico-mechanical properties, changes in color and gloss should be taken into account.

2. Materials and Methods

2.1. Material

In this study, five different natural stone samples of sedimentary origin were used. A total of 150 samples, 30 of each rock type, were exposed to different temperatures. The location map of samples used in the experimental study is given in Figure 1. The codes, trade names and origins of the samples are given in Table 1. The 30 × 40 × 40 mm-sized samples were prepared to determine the physico-mechanical properties of natural stones. Test samples and devices are given in Figure 2a–f.

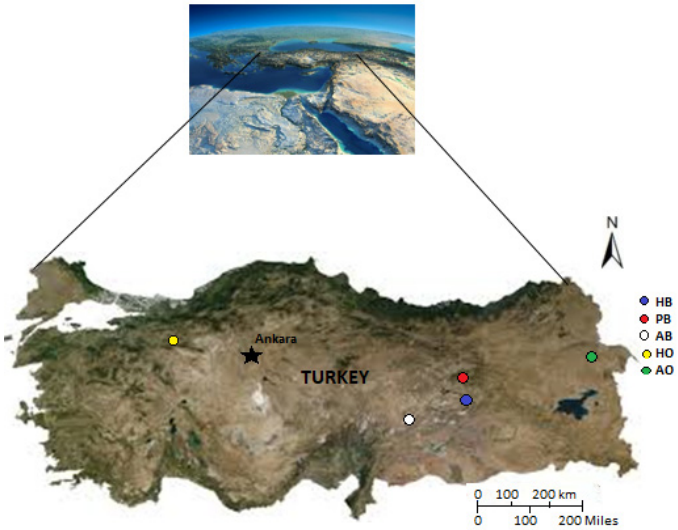

Figure 1. Location map of samples.

Table 1. Codes, trade names and origins of natural stones.

Code	Commercial Name	Stone Type	Location
HB	Hazar Beige	Limestone	Hazar-Elazig
PB	Pertek Beige	Limestone	Pertek-Tunceli
AB	Akçadağ Beige	Limestone	Akçadağ-Malatya
HO	Honey Onyx	Limestone	Sögüt-Bilecik
AO	Ağrı Onyx	Dolomite	Diyadin-Ağri

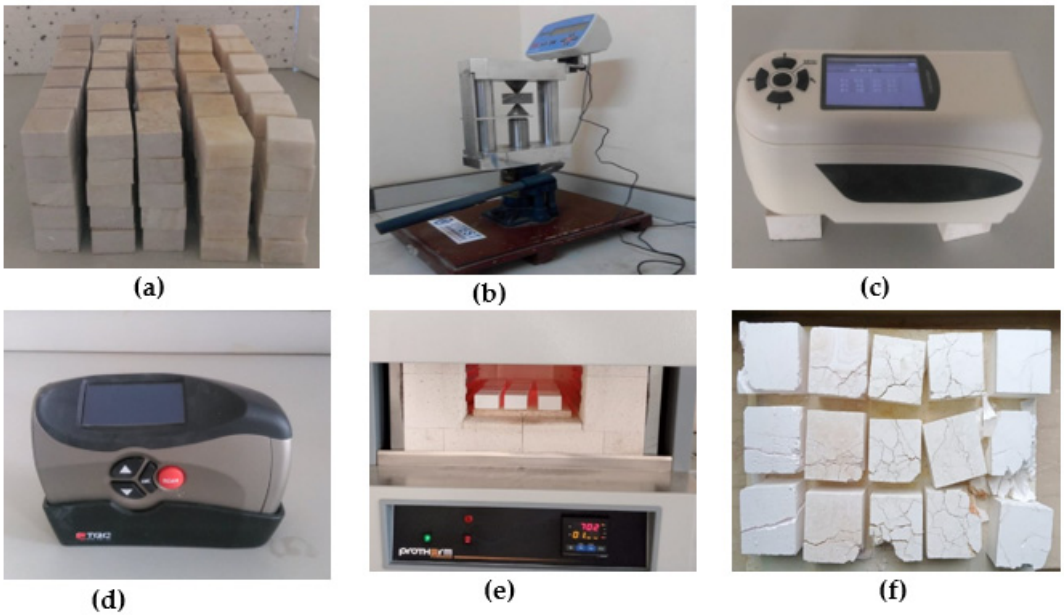

Figure 2. (**a**) Test samples, (**b**) Point load test device, (**c**) Colorimeter, (**d**) Gloss meter, (**e**) Samples being exposed to temperature and (**f**) Samples exposed to 1000 °C.

2.2. Methods

2.2.1. High Temperature Test

Samples at room temperature (i.e., not exposed to any temperature) were accepted as reference samples. Then, other samples were compared with the reference samples after exposure to each temperature. In the current literature, laboratory ovens are most commonly used to determine the effect of fire on natural stones. In order to explain the effect of temperature, temperature values were preferred in different ranges. The purpose of choosing different temperature values is to clearly see changes occurring in each temperature range. The highest temperature value used in the study was selected as 1000 °C. However, measurements could not be taken due to the natural stones being broken at this temperature (see Figure 2f). The experimental study was conducted by exposing samples to five different temperature values (23, 200, 400, 600 and 800 °C). Using a Protherm PLF model oven, each temperature value was adjusted by considering the heating rate of the oven. Thus, the natural stones were exposed to required high temperatures. After reaching the specified temperature, the natural stones remained at that temperature in the oven for 120 min. Natural stones exposed to high temperatures were kept in the oven until they were at room temperature in order to avoid sudden thermal shock. After the samples reached room temperature, non-destructive tests (water absorption, porosity, color, gloss, Schmidt hammer hardness) were performed, and then point load strength was determined.

2.2.2. Non-Destructive Tests

Non-destructive tests are highly preferred due to being fast, easy and practical in studies related to earth sciences. In this study, non-destructive tests (water absorption, porosity, color, gloss, Schmidt hammer hardness) were applied before determining the

point load strength of the samples. For the water absorption and porosity of the rocks, 5 samples with dimensions of 70 × 70 × 70 mm were used. Water absorption by weight and apparent porosity were determined according to TS EN 13755 and TS EN 1936, respectively [25,26]. For this purpose, the dry, saturated weights and volumes of the samples were determined. The water absorption and porosity values of the rocks were determined by using Equations (1) and (2).

$$Aw = \frac{Ws - Wd}{Wd} \quad (1)$$

$$P = \frac{Ws - Wd}{V}\% \quad (2)$$

where Aw: Water absorption by weight (%), Ws: Saturated sample (gr), Wd: Dry sample (gr), P: Porosity (%) and V: Volume (cm^3).

The Schmidt hammer is a fast and inexpensive test that is widely used to predict material properties of rocks such as uniaxial compressive strength and Young's modulus. The Schmidt hammer is divided into L and N types with different impact energies. The L-type hammer is most commonly used to estimate uniaxial compressive strength and Young's modulus [27]. An L-type Schmidt hammer with an impact energy of 0.74 Nm was used to determine Schmidt hammer hardness values. Measurements were taken 20 times from different points of each cubic sample and evaluated according to the method suggested by Aydin [28]. Accordingly, the arithmetic mean of the highest 10 values was accepted as the Schmidt hammer hardness of rock.

A subjective assessment of color measurement by eye can sometimes be misleading. For this reason, objective measurements made with various devices are required. It has become common to evaluate color and color differences instrumentally according to the method developed by the International Lighting Commission. This method is known as the CIELAB (L*, a*, b*) three-point measurement [29]. The coordinate system of colors is given in Figure 3. In this system, L* is the degree of darkness and lightness of color on a scale ranging from white (L* = 100) to black (L* = 0), a* is the scale on the axis ranging from green (−a*) to red (+a*) and b* is the scale on the axis ranging from blue (−b*) to yellow (+b*). Color changes occurring at different temperatures were determined by the Hunter CIELAB colorimeter. In this study, the NR200 colorimeter, introduced by 3nh, which has passed tens of thousands of tests and applied many innovative technologies, was used. The arithmetic averages were obtained by measuring from four different points around the midpoint of each sample.

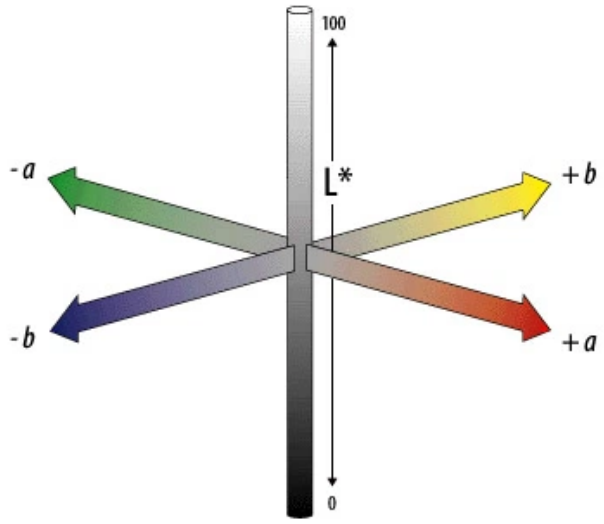

Figure 3. Coordinate system for CIELAB.

A beam of light shining onto a bright surface is theoretically refracted at the angle it came from. Thus, gloss is the reflected amount of beam coming to the surface at a certain angle, expressed as a percentage (%) relative to the gloss of glass with a refractive index of 1.57. Gloss measurements are made by sending the light at angles of 20, 45, 60 and 85 degrees [30]. This study is based on measurements made at an angle of 60°. Changes of gloss occurring at different temperatures were determined using the Q TQC GL0010 digital gloss meter (Range: 0–2000 GU; Repeatability r*: 0.2 GU; Reproducibility R*: 1.6 GU and Bias: 0.6 GU). The arithmetic averages were obtained by measuring from four different points around the midpoint of each sample. Measured values were obtained in GU (gloss units).

2.2.3. Point Load Strength Test

The uniaxial compressive strength of rocks is the most preferred mechanical test in earth science projects such as mining and civil engineering. This test requires time-consuming, expensive equipment, uniformly geometrically shaped specimens and skilled personnel [31–33]. However, in some situations where time is limited and sufficient samples cannot be obtained, it is easier to use the point load strength suggested by ISRM 1985 [34]. Point load strength is a simple, fast and inexpensive index test method that can be applied both in the field and in the laboratory. To determine this strength, core samples (for diametric and axial tests), cut block samples or irregular-sized samples can be used [35,36]. In this study, cut block samples were preferred. The experimental study was conducted according to the method recommended by ISRM 1985 [34]. The tests were conducted using a Digital Point Load Tester (UTEST-UTR-0580 model) that has a 60 kN capacity test body and a digital readout unit loaded with a hydraulic hand pump. For this purpose, 30 × 40 × 40 mm-sized samples were prepared. To determine the point load strength of the natural stones, firstly the uncorrected point loading strength is calculated by Equation (3).

$$Is = \frac{P}{De^2} \tag{3}$$

where Is is uncorrected point load strength (MPa), P is failure load (kN, kgf, etc.) and De is equivalent core diameter (mm).

Equivalent core diameter is calculated by Equation (4) for cut block samples.

$$De^2 = \frac{4A}{\pi} \tag{4}$$

where A is the smallest cross-sectional area of the sample passing through contact points of conical heads. Corrected point loading strength is calculated by Equations (5) and (6).

$$F = \left(\frac{De}{50}\right)^{0.45} \tag{5}$$

$$Is_{(50)} = F \times Is \tag{6}$$

where $Is_{(50)}$ is corrected point load strength (MPa) and F is correction factor.

3. Results and Discussion

The XRF results of the samples used in the experimental study are given in Table 2, and the XRD results are given in Figure 4. While the main minerals of the AO sample are limestone and dolomite, other samples contain limestone. Since all samples are resistant to 800 °C, measurements could not be taken at higher temperatures. As a result of each temperature, water absorption, porosity, Schmidt hammer hardness and point load strength were recorded for each natural stone. These values of the samples obtained at different temperatures are given in Table 3. The percentage change in temperature-related physico-mechanical properties is given in Table 4. As can be clearly seen in Table 4, as the temperature value increased, it led to an increase in the water absorption and porosity

and also a decrease in the Schmidt hammer hardness and point load strength of all natural stones. These changes vary among natural stones; for this reason, each experimental parameter was considered separately.

Table 2. Results of XRF analysis of samples.

Sample	HB (%)	PB (%)	AB (%)	HO (%)	AO (%)
Fe_2O_3	0.06	0.06	0.15	2.45	1.66
MgO	0.45	0.42	0.30	0.69	14.48
Al_2O_3	0.04	0.04	0.08	<0.01	<0.01
SiO_2	<0.01	<0.01	<0.01	<0.01	<0.01
P_2O_5	<0.01	<0.01	0.01	0.06	0.07
K_2O	<0.01	<0.01	<0.01	0.01	0.01
CaO	54.14	53.15	53.70	52.16	38.82
TiO_2	<0.01	<0.01	0.01	<0.01	<0.01
MnO	<0.01	<0.01	<0.01	0.29	0.35
ZnO	<0.01	<0.01	<0.01	<0.01	<0.01
SrO	0.02	0.02	0.01	<0.01	<0.01
PbO	<0.01	<0.01	<0.01	<0.01	<0.01
Na_2O	2.20	2.18	2.01	0.08	0.12
LOI	43.08	44.12	43.73	44.25	44.48

(LOI: Loss on ignition).

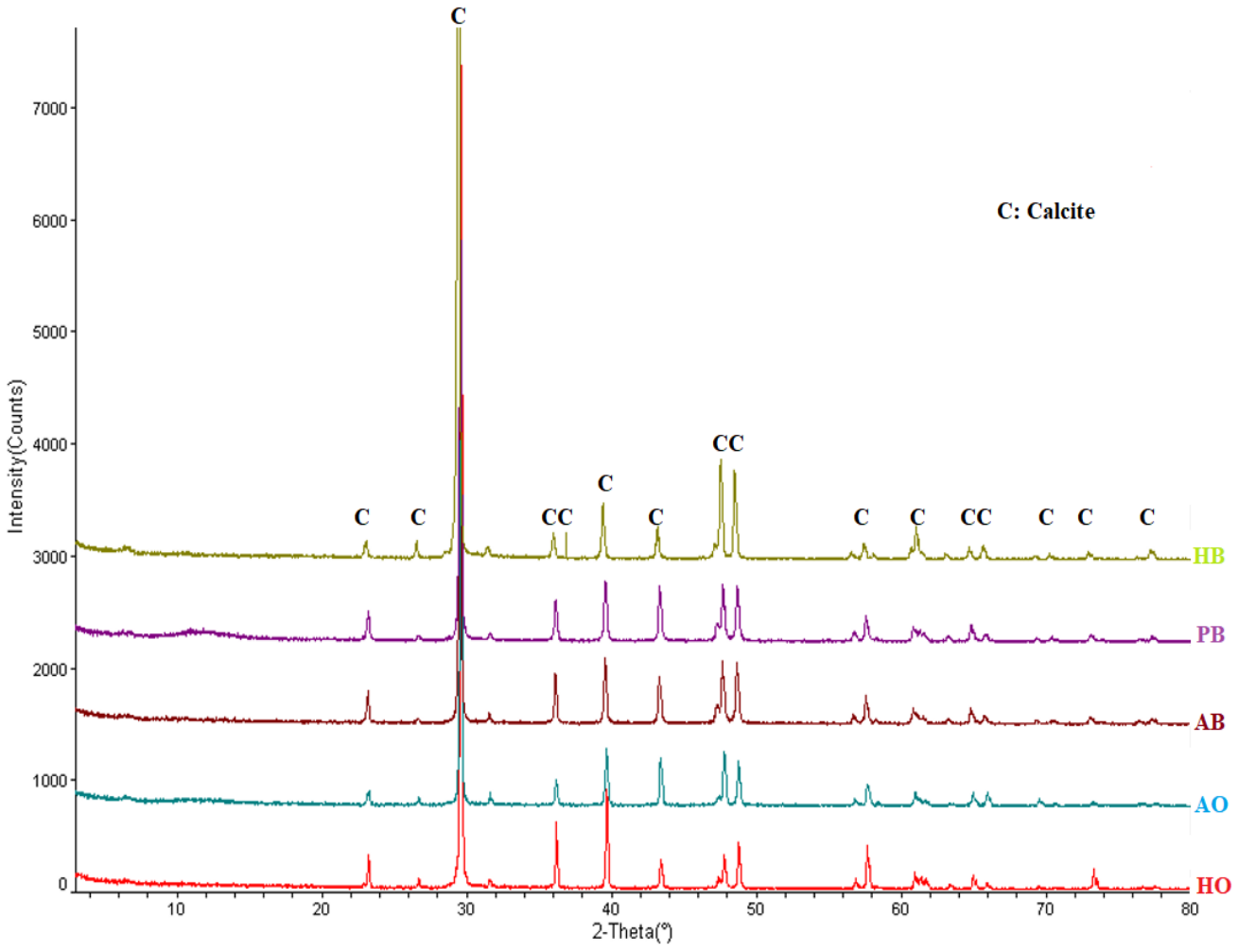

Figure 4. XRD chart of natural stones.

Table 3. Average results of physico-mechanical properties at different temperatures.

Test	Code	23 °C	200 °C	400 °C	600 °C	800 °C
Water Absorption (%)	HB	0.162 ± 0.031	0.164 ± 0.034	0.587 ± 0.053	1.008 ± 0.088	4.862 ± 0.245
	PM	0.158 ± 0.030	0.161 ± 0.037	0.787 ± 0.062	1.321 ± 0.101	5.142 ± 0.271
	AB	0.151 ± 0.032	0.155 ± 0.040	0.889 ± 0.069	1.719 ± 0.124	6.541 ± 0.432
	HO	0.202 ± 0.048	0.210 ± 0.044	0.907 ± 0.078	2.388 ± 0.142	9.643 ± 0.678
	AO	0.221 ± 0.042	0.229 ± 0.042	0.972 ± 0.101	2.524 ± 0.159	10.862 ± 0.702
Porosity (%)	HB	0.466 ± 0.058	0.472 ± 0.054	1.702 ± 0.122	2.993 ± 0.171	13.965 ± 0.897
	PM	0.422 ± 0.050	0.451 ± 0.051	2.423 ± 0.154	3.976 ± 0.192	15.785 ± 0.991
	AB	0.423 ± 0.048	0.433 ± 0.049	2.777 ± 0.158	5.570 ± 0.298	20.221 ± 1.131
	HO	0.589 ± 0.062	0.601 ± 0.060	2.884 ± 0.170	7.593 ± 0.542	24.294 ± 1.211
	AO	0.652 ± 0.060	0.672 ± 0.062	3.120 ± 0.181	8.134 ± 0.612	25.784 ± 1.227
Schmidt Hammer Hardness	HB	45.4 ± 0.6	45.3 ± 0.7	44.2 ± 0.7	40.4 ± 0.6	20.6 ± 0.4
	PM	44.8 ± 0.5	44.6 ± 0.6	43.0 ± 0.7	39.2 ± 0.7	19.2 ± 0.4
	AB	43.1 ± 0.5	43.0 ± 0.6	42.1 ± 0.6	36.2 ± 0.4	18.5 ± 0.3
	HO	38.4 ± 0.4	38.3 ± 0.4	37.4 ± 0.5	32.9 ± 0.5	13.8 ± 0.3
	AO	37.1 ± 0.5	37.0 ± 0.4	35.9 ± 0.6	29.8 ± 0.4	11.4 ± 0.2
Point Load Strength (MPa)	HB	7.67 ± 0.89	7.64 ± 0.63	7.01 ± 0.56	4.61 ± 0.37	2.24 ± 0.11
	PM	7.58 ± 0.33	7.53 ± 0.46	6.82 ± 0.48	4.02 ± 0.34	1.18 ± 0.12
	AB	5.89 ± 0.17	5.87 ± 0.47	4.91 ± 0.36	3.58 ± 0.29	1.42 ± 0.14
	HO	5.49 ± 0.32	5.44 ± 0.36	4.51 ± 0.32	3.18 ± 0.26	1.04 ± 0.19
	AO	5.21 ± 0.46	5.20 ± 0.41	5.06 ± 0.44	3.02 ± 0.14	0.82 ± 0.11

Table 4. The percentage change in temperature-related physico-mechanical properties.

Test	Heat (°C)	HB (%)	PB (%)	AB (%)	HO (%)	AO (%)
Water Absorption	200	+0.002	+0.003	+0.004	+0.008	+0.008
	400	+0.425	+0.629	+0.738	+0.705	+0.751
	600	+0.846	+1.163	+1.568	+2.186	+2.303
	800	+4.700	+4.984	+6.390	+9.441	+10.641
Porosity	200	+0.006	+0.029	+0.010	+0.012	+0.020
	400	+1.236	+2.001	+2.354	+2.295	+2.468
	600	+2.527	+3.554	+5.147	+7.004	+7.482
	800	+13.499	+15.363	+19.798	+23.705	+25.132
Schmidt Hammer Hardness	200	−0.220	−0.446	−0.232	−0.260	−0.270
	400	−2.643	−4.018	−2.320	−2.604	−3.235
	600	−11.013	−12.500	−16.009	−14.323	−19.677
	800	−54.626	−57.143	−57.077	−64.063	−69.272
Point Load Strength	200	−0.391	−0.660	−0.340	−0.911	−0.192
	400	−8.605	−10.026	−16.638	−17.851	−2.879
	600	−39.896	−46.966	−39.219	−42.077	−42.035
	800	−70.795	−84.433	−75.891	−81.056	−84.261

(+: Increase; −: Decrease).

Many researchers have determined that there is a strong relationship between water absorption and porosity [37,38]. This strong relationship is clearly seen in this study as well. Changes in porosity and water absorption values of natural stones due to high temperatures are parallel to each other. The result of water absorption values measured from samples exposed gradually to high temperatures from room temperature up to 800 °C is given in Figure 5. When Figure 5 is analyzed, it is seen that water absorption values of samples up to 400 °C do not change significantly with temperature. However, it is seen that all samples are highly affected when this temperature value increases gradually. A similar situation was discussed by Ferrero and Marini (2001) in their study on how high temperatures affect physical properties of rocks [39].

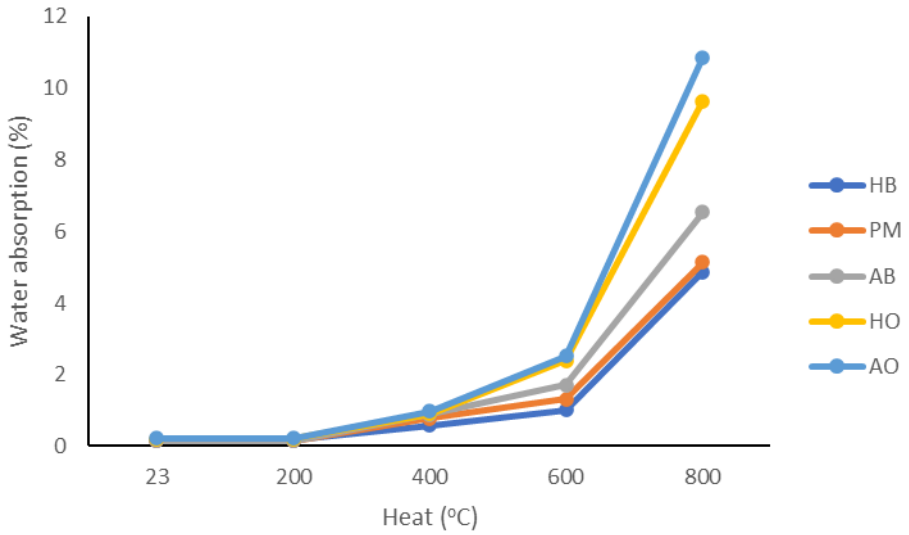

Figure 5. Water absorption change related to temperature.

There is generally an inverse relationship between the porosity and strength of natural stones. In other words, as the porosity of natural stones increases, its strength decreases. However, it is known that pore shape, pore size and spatial distribution are also important. Pores may occur at grain boundaries and within the grain of natural stones [40]. Therefore, a comprehensive pore study can be useful to determine how natural stones are affected by exposure to bad environmental conditions (freeze–thaw, high temperature, wetting–drying, salt crystallization, etc.). Porosity values of the samples subjected gradually to high temperatures, from room temperature (23 °C) to 800 °C, are given in Figure 6. As can be clearly seen in Figure 6, each gradual increase in temperature increased the porosity of the natural stones. It is seen that the porosity increase in onyx is higher than in limestone. As the temperature increases, the porosity of the HB sample is lower than other natural stones. In all natural stones, porosity increases suddenly at temperatures above 400 °C. Especially after this temperature, the porosity of the HO and AO samples increases dramatically. Many researchers state that there is a linear relationship between porosity and temperature, and the higher the temperature, the greater the porosity. The increase in porosity is more obvious at temperatures of 400 °C and above [41–43]. Gomez-Heras et al. (2006) reveal that the porosity of certain rocks increases due to an increase in temperature. Similar results were obtained in this study [44].

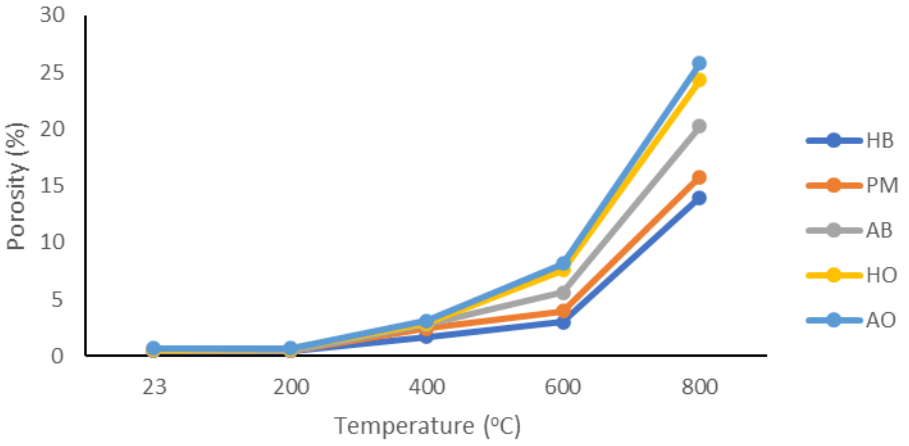

Figure 6. Porosity changes related to temperature.

Schmidt hammer hardness is a very important parameter in the investigation of high temperature effects on natural stones, since it is a non-destructive test and is used to predict

the mechanical strength of rocks. In this study, it contributes to the evaluation of the mechanical strength of natural stone as a result of a possible fire (high temperature) using a non-destructive testing method of Schmidt hardness hammer. Schmidt hammer hardness values of samples subjected to high temperatures, from room temperature (23 °C) to 800 °C, are given in Figure 7. It is clear that, as the temperature value increases, the Schmidt hammer hardness results are negatively affected. In particular, at the critical temperature of 600 °C, there were significant decreases in the Schmidt hammer hardness of all samples. At 800 °C, the biggest Schmidt hardness loss is in the HO and AO samples, with 64.1% and 69.3%, respectively, and the smallest loss is in HB sample, with 54.6%. The formation of new micro–macro cracks, fracture and distortion with the increase in temperature negatively affected the Schmidt hammer hardness values of rocks. Many researchers have obtained strong relationships between mechanical properties and Schmidt hammer hardness as a result of experimental and statistical studies [45–47]. In this case, when considering the strong relationship between Schmidt hammer hardness and mechanical properties (uniaxial compression, impact, bending strength, etc.), it is obvious that such a high loss cannot be ignored.

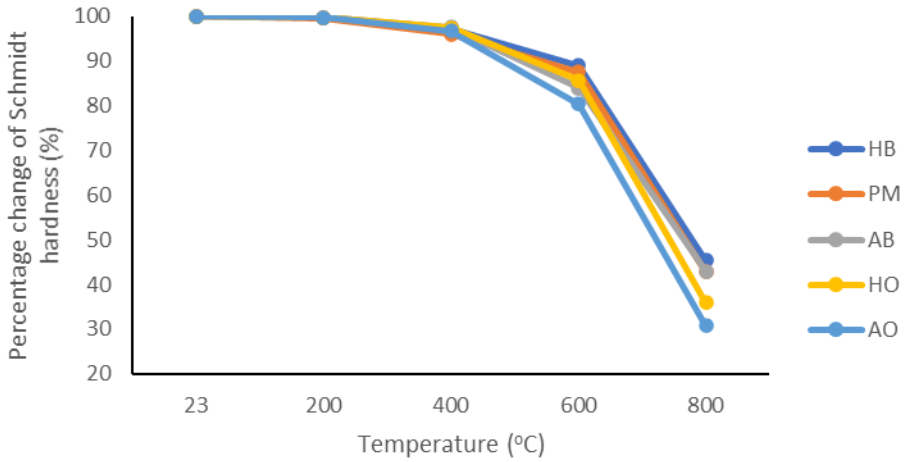

Figure 7. Schmidt hammer hardness change related to temperature.

The point load strength values of samples subjected to high temperatures, from room temperature (23 °C) to 800 °C, are given in Figure 8. As can be clearly seen in Figure 8, in limestone and onyx samples at temperatures above 400 °C, a remarkable decrease was observed in the strength of samples when compared with their initial point load strength at room temperature. This result is also related to the change in water absorption and porosity of the natural stones due to an increase in temperature. It is known that formation of new micro cracks and pores causes strength loss of natural stones. The increase in porosity makes natural stones less compact and consequently leads to loss of strength [48]. When Figure 8 is examined, it is seen that point load strength of all natural stones decreases due to an increase in porosity. In particular, it is clear that a high increase in the porosity of HO and AO samples significantly reduces their point load strength values. At 800 °C, the biggest point load strength loss is in PM and AO samples, with 84.4% and 84.2%, respectively, and the smallest loss is in the HB sample, with 70.8%. However, if it is necessary to make a general evaluation, it is seen that strength loss is over 70% in all samples. This shows that exposure of all natural stones used in this experimental study to such high temperatures may be inconvenient. The main reason for this is that elements and compounds in organic groups, such as C, H_2, N_2 and S_2, and inorganic groups, such as $CaCO_3$, $CaSO_4$ and Ca $(OH)_2$ undergo chemical changes during fires, causing the molecular structure of the material to deteriorate. In particular, this phenomenon can be encountered in some natural stone structures containing fossils. During the degradation of the molecular structure of the material, some harmful gases, such as CO_2, CO, SO_2 and SO_3, may occur; these gases

leave the body of the material and create chemical deformations. This change may differ according to the mineral components forming the natural stone [49–51]. Similar results were obtained in this study.

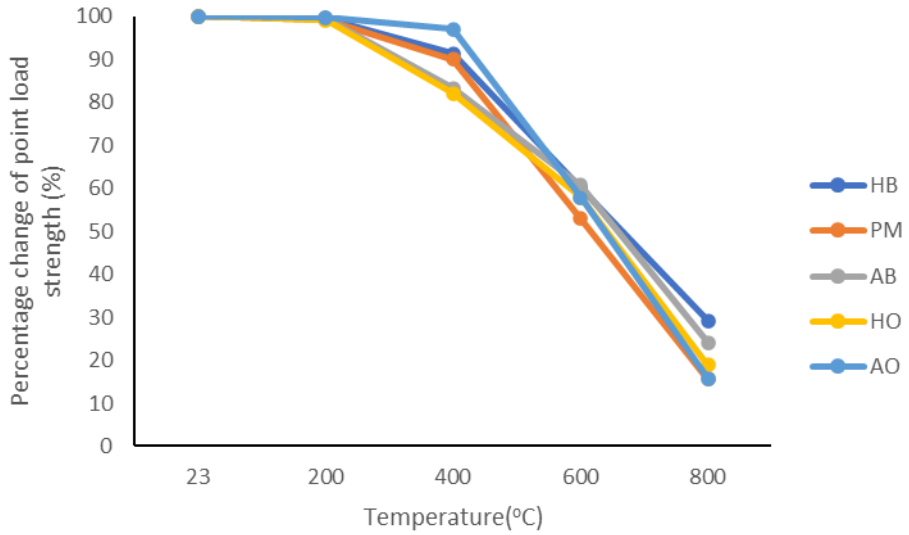

Figure 8. Point load strength values change related to temperature.

The average color and gloss values of the natural stones are given in Table 5. The color L*, a* and b* values on surfaces of the natural stone samples exposed to different temperatures are shown in Figure 9a–c. As can be seen in Figure 9a, while all samples darkened at 400 °C, the color of the samples became lighter with an increase in temperature. While the original surface whiteness value (L*) of the natural stones was 71.94–83.77, it was between 81.17–93.93 after the application of 800 °C. This situation may have increased the whiteness of the surface due to the decomposition of the sample at this temperature. Surface redness values (a*) of the samples after applying different temperatures are shown in Figure 9b. Except for HO and AO samples, other samples changed from red to green after 600 °C. The fact that the redness value (a*) approaches zero indicates that the surface of the sample is whitening. Although HO and AO samples do not change to green, their redness is reduced. It is thought that the fluctuation in the redness value of the HO sample may be due to Fe_2O_3 content. A similar situation is observed in the WO sample. However, the fluctuation is more in the HO sample with a high Fe_2O_3 content. As can be seen in Figure 9c, the surface yellowness value (b*) decreases significantly as a result of the high temperature applied to samples. The surface yellowness value of the HO sample was less affected than the others. The HM and PM samples changed from yellow to blue after the application of 800 °C. Gloss values of the samples subjected gradually to high temperatures, from room temperature (23 °C) to 800 °C, are given in Figure 9d. When gloss values were examined, it was observed that the gloss of the natural stone samples varied between 98.4–55.6 GU. While the highest brightness value was obtained from the HO sample (98.4 GU), this sample was followed by PM (74.6 GU), HB (74.1 GU), AO (56.4 GU) and AB (55.6 GU), respectively (Table 5). It was observed that gloss values changed slightly (6.5–23.9%) at temperatures up to 400 °C, and increased rapidly (55.4–84.5%) at 800 °C. The reason for this change is that the surfaces of natural stones are warmed up quickly and expand in volume due to the high temperature. As a result, the surface tension of the samples increases and creates micro or macro cracks on their surfaces. The visual appearance of color changes occurring on natural stone surfaces at different temperatures is given in Figure 10.

Table 5. Average of color and gloss values at different temperatures.

Code	L*, a*, b*, GU	23 °C	200 °C	400 °C	600 °C	800 °C
HB	L	74.09	72.87	69.67	70.15	88.11
	a	3.89	3.94	4.20	2.75	−2.01
	b	10.12	10.41	9.81	5.67	−4.15
	GU	74.1	73.2	68.2	60.3	26.3
PM	L	79.15	77.58	57.25	63.87	84.77
	a	3.77	4.07	3.13	3.10	−1.38
	b	12.32	12.28	8.08	6.07	−2.25
	GU	94.6	91.8	88.5	75.3	26.0
AB	L	72.54	71.22	55.42	61.72	81.17
	a	6.91	6.46	4.64	4.28	−0.75
	b	17.01	16.95	8.01	7.83	1.06
	GU	55.6	51.8	48.3	43.9	24.8
HO	L	71.94	73.51	69.86	79.77	92.98
	a	3.05	2.41	4.02	1.62	2.31
	b	8.02	11.8	11.8	4.66	5.38
	GU	98.4	95.8	91.1	52.4	15.3
AO	L	83.77	86.85	81.53	87.45	98.93
	a	1.28	1.15	1.59	1.33	0.69
	b	3.86	5.04	6.47	3.29	−0.48
	GU	56.4	45.9	42.9	22.3	12.1

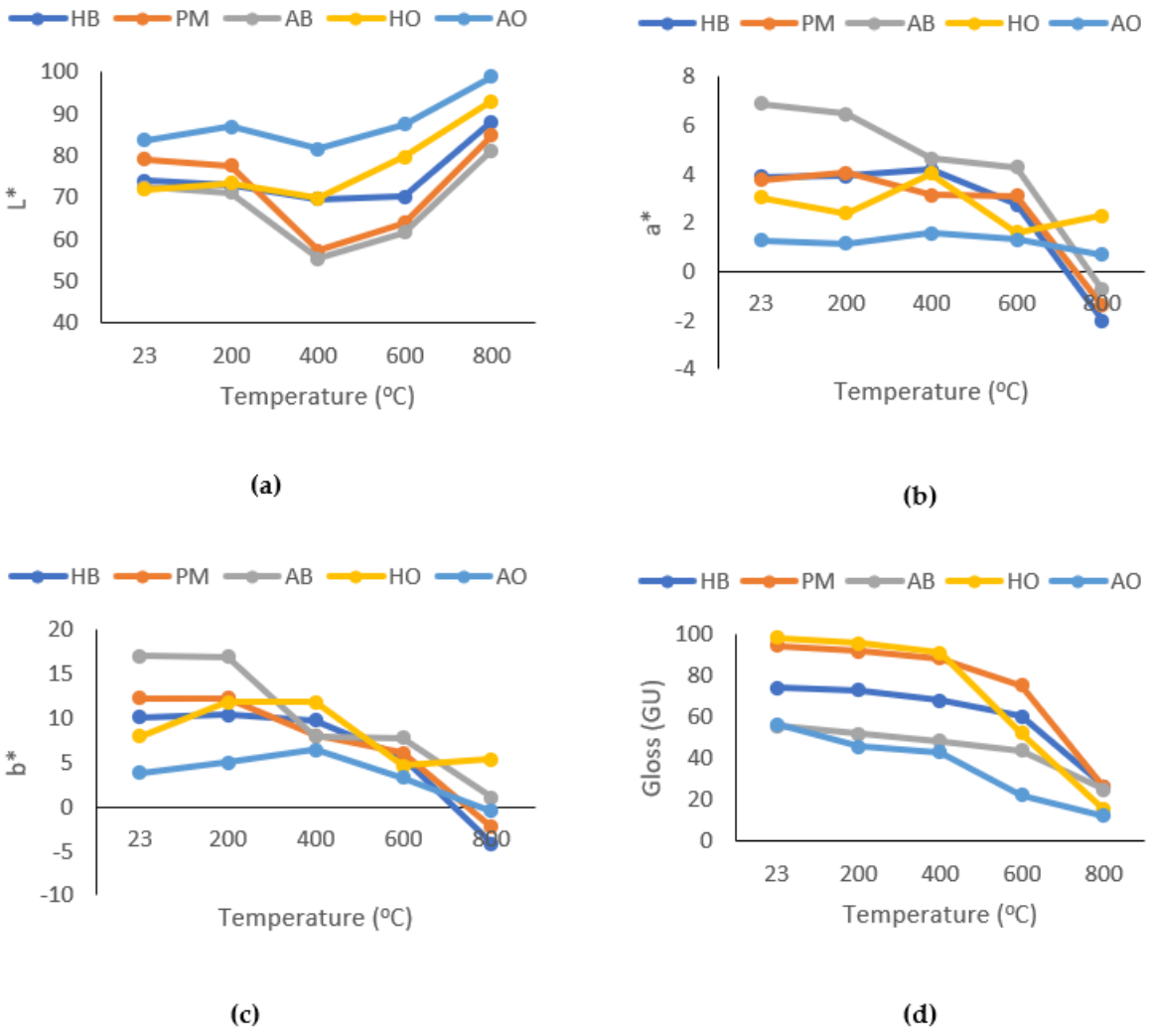

Figure 9. The color and gloss values of samples.

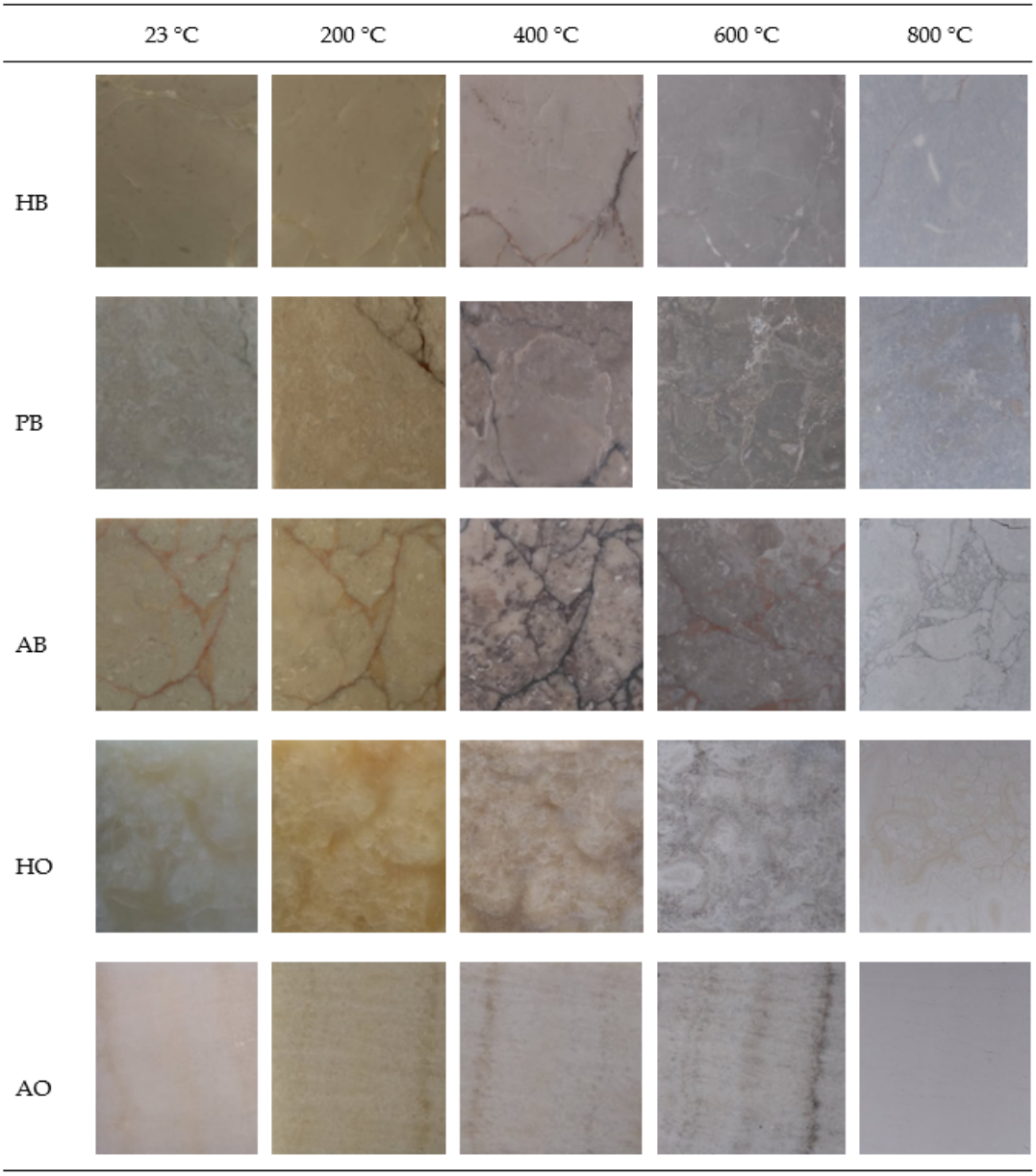

Figure 10. Visual appearance of color changes.

It is important for restoration studies to consider the color changes while examining the changes in properties of natural stones exposed to fire. In fact, color changes are a clue to determine what temperature building blocks are exposed to during fire. This study shows that there is a color change on the surfaces of natural stones at different temperatures. Color changes of natural stones exposed to different temperatures are given in Figure 10. When the sample surfaces are examined, it is seen that it darkens up to 400 °C, which is the turning point. However, it is seen that the white color dominates, depending on the temperature increase after 400 °C. The color change was mostly seen in the HO and AO samples.

4. Conclusions

In this study, five different light-colored natural stone samples (limestone and onyx) were exposed to different temperatures (from room temperature to 800 °C) and some physico-mechanical properties (water absorption, porosity, Schmidt hammer hardness and

point load strength) and color and gloss values were determined. The following results were obtained.

Although the highest temperature used in the study was chosen as 1000 ºC, all samples were broken down at this temperature. Therefore, measurements could not be taken at this temperature.

The physico-mechanical properties of samples exposed to temperatures up to 400 °C were not affected much. This temperature value can also be called the mutation point.

After 400 °C, sudden increases in water absorption and porosity values of all samples were determined. Especially after this temperature, water absorption and porosity of HO and AO samples increase dramatically. This situation is caused by newly formed capillary cracks due to the increasing temperature.

For Schmidt hammer hardness, the critical temperature was determined to be 600 °C. After this temperature, there is a dramatic decrease in hardness values of all samples. In particular, an almost 64–69% decrease was determined in the Schmidt hardness values of onyx samples.

As the temperature value increased, porosity and water absorption values of the samples increased. Therefore, the point load strength of the samples was affected negatively. In particular, point load strength values of samples at 600 °C and above dramatically decrease. In fact, the LOI from the XRF analysis supports these results.

In general, all samples darkened at 400 °C, while the whiteness value (L*) of samples increased at the 800 °C. The highest whiteness value was obtained at 1000 °C. However, measurements were not taken because other physico-mechanical properties could not be determined.

At exposure to 800 °C, the surface gloss of HO was greatly reduced (83 GU), while the BO sample was affected less (44 GU). However, when evaluated as a percentage, the surface gloss loss of the PM and HB samples is less than other samples.

As temperatures increased, the surface redness value (a*) of all samples decreased at varying rates, and this value of the HO sample decreased to a minimal level compared to the others. It is thought that fluctuation in the redness value of the HO sample may be due to Fe_2O_3 content. A similar situation is observed in the WO sample. However, the fluctuation is greater in the HO sample with a high Fe_2O_3 content.

The biggest advantage of color determination is that it gives information about the temperature the natural stone is exposed to during fires.

As a result, natural stones used in many areas are required to maintain their durability, gloss and color for long periods. For this, not only physico-mechanical properties of natural stones, but also the most suitable usage areas should be recognized. Considering the results of this study, temperatures of 600 °C and above caused destructive damage for all samples. Therefore, a large amount of loss in physico-mechanical strength of the samples can damage the building structure and also increase the cost of restoration. In addition, fire is generally effective on all types of materials. However, determining the burning time and maximum temperature to which rock is exposed during a fire is very important in the restoration of structures. It is seen that strength loss of natural stones is insignificant up to 400 °C, but there is a darkening in surface color. In the restoration of a structure exposed to such a fire, it is useful to focus on surface polishing rather than strength.

Funding: This research received no external funding.

Institutional Review Board Statement: Not applicable.

Informed Consent Statement: Not applicable.

Data Availability Statement: Data presented in this research paper can be obtained from the corresponding author upon request.

Acknowledgments: I appreciate helpful suggestions from this journal's reviewers.

Conflicts of Interest: The author declares that there is no conflict of interest.

References

1. Celik, M.Y. Types and usage areas of the decorative natural building stones. *Sci. Min. J.* **2003**, *42*, 3–15. (In Turkish)
2. Karakaş, A.; Morali, G.; Coruk, Ö.; Bozkurtoğlu, E. Geomechanical, durability–hygrothermal and thermal shock properties of Kocaeli Kandira stone used as building stone in historical structures. *Environ. Earth Sci.* **2021**, *80*, 130. [CrossRef]
3. Mutlutürk, M.; Altindag, R.; Türk, G. A decay function model for the integrity loss of rock when subjected to recurrent cycles of freezing-thawing and heating-cooling. *Int. J. Rock Mech. Min. Sci.* **2004**, *41*, 237–244. [CrossRef]
4. Yavuz, H. Effect of freeze–thaw and thermal shock weathering on the physical and mechanical properties of an andesite stone. *Bull. Eng. Geol. Environ.* **2011**, *70*, 187–192. [CrossRef]
5. Fener, M.; Ince, I. Effects of the freeze–thaw (F-T) cycle on the andesitic rocks (Sille-Konya/Turkey) used in construction building. *J. African Earth Sci.* **2015**, *109*, 96–106. [CrossRef]
6. Ghobadi, M.H.; Babazadeh, R. Experimental studies on the effects of cyclic freezing-thawing, salt crystallization, and thermal shock on the physical and mechanical characteristics of selected sandstones. *Rock Mech. Rock Eng.* **2015**, *48*, 1001–1016. [CrossRef]
7. Gökçe, M.V.; İnce, İ.; Fener, M.; Taşkıran, T.; Kayabali, K. The effects of freeze–thaw (F-T) cycles on the Gödene travertine used in historical structures in Konya (Turkey). *Cold Reg. Sci. Tech.* **2016**, *127*, 65–75. [CrossRef]
8. Bozdağ, A.; Bayram, A.F.; İnce, İ.; Asan, K. The relationship between weathering and welding degree of pyroclastic rocks in the Kilistra ancient city, Konya (Central Anatolia, Turkey). *J. African Earth Sci.* **2016**, *123*, 1–9. [CrossRef]
9. Heidari, M.; Torabi-Kaveh, M.; Mohseni, H. Assessment of the effects of freeze–thaw and salt crystallization ageing tests on Anahita Temple Stone, Kangavar, West of Iran. *Geotech. Geol. Eng.* **2017**, *35*, 121–136. [CrossRef]
10. Özşen, H.; Bozdağ, A.; İnce, İ. Effect of salt crystallization on weathering of pyroclastic rocks from Cappadocia, Turkey. *Arab. J. Geosci.* **2017**, *10*, 258. [CrossRef]
11. Deng, H.; Yu, S.; Deng, J. Damage characteristics of sandstone subjected to coupled effect of freezing-thawing cycles and acid environment. *Adv. Civ. Eng.* **2018**, *2018*, 3560780. [CrossRef]
12. Sun, Q.; Zhang, Y. Combined effects of salt, cyclic wetting and drying cycles on the physical and mechanical properties of sandstone. *Eng. Geol.* **2019**, *248*, 70–79. [CrossRef]
13. Amirkiyaei, V.; Ghasemi, E.; Faramarzi, L. Determination of P-wave velocity of carbonate building stones during freeze–thaw cycles. Geotech. *Geol. Eng.* **2020**, *38*, 5999–6009.
14. Guler, S.; Türkmenoğlu, Z.F.; Varol, O.O. Thermal shock and freeze–thaw resistance of different types of carbonate rocks. *Int. J. Rock Mech. Min. Sci.* **2021**, *137*, 104545. [CrossRef]
15. Mardoukhi, A.; Mardoukhi, Y.; Hokka, M.; Kuokkala, V.T. Effects of test temperature and low temperature thermal cycling on the dynamic tensile strength of granitic rocks. *Rock Mech. Rock Eng.* **2021**, *54*, 443–454. [CrossRef]
16. Goudie, A.S.; Allison, R.J.; McLaren, S.J. The relations between modulus of elasticity and temperature in the context of the experimental simulation of rock weathering by fire. *Earth Surf. Proc. Landf.* **1992**, *17*, 605–615. [CrossRef]
17. Allison, R.J.; Bristow, G.E. The effects of fire on rock weathering: Some further considerations of laboratory experimental simulation. *Earth Surf. Proc. Landf.* **1999**, *24*, 707–713. [CrossRef]
18. Chakrabarti, B.; Yates, T.; Lewry, A. Effect of fire damage on natural stonework in buildings. *Constr. Build. Mater.* **1996**, *10*, 539–544. [CrossRef]
19. Sippel, J.; Siegesmund, S.; Weiss, T.; Nitsch, K.H.; Korzen, M. Decay of natural stones caused by fire damage. *Geol. Soc. Lond. Spec. Publ.* **2007**, *271*, 139–151. [CrossRef]
20. Hajpál, M.; Török, Á. Mineralogical and colour changes of quartz sandstones by heat. *Environ. Geol.* **2004**, *46*, 311–322. [CrossRef]
21. Gillhuber, S.; Lehrberger, G.; Goske, J. Fire damage of trachyte: Investigations of the Tepla monastery building stones. *Geol. Soc. Lond. Spec. Publ.* **2010**, *333*, 73–79. [CrossRef]
22. Hajpál, M. Changes in sandstones of historical monuments exposed to fire or high temperature. *Fire Technol.* **2002**, *38*, 373–382. [CrossRef]
23. Tian, H.; Ziegler, M.; Kempka, T. Physical and mechanical behavior of claystone exposed to temperatures up to 1000 °C. *Int. J. Rock Mech. Min. Sci.* **2014**, *70*, 144–153. [CrossRef]
24. Ozguven, A.; Ozcelik, Y. Effects of high temperature on physico-mechanical properties of Turkish natural building stones. *Eng. Geol.* **2014**, *183*, 127–136. [CrossRef]
25. *TS EN 13755*; Natural Stone Test Methods—Determination of Water Absorption at Atmospheric Pressure. Turkish Standardization Institute: Ankara, Turkey, 2009. (In Turkish)
26. *TS EN 1936*; Natural Stone Test Methods—Determination of Real Density and Apparent Density and of Total and Open Porosity. Turkish Standardization Institute: Ankara, Turkey, 2010. (In Turkish)
27. Wang, M.; Wan, W. A new empirical formula for evaluating uniaxial compressive strength using the Schmidt hammer test. *Int. J. Rock Mech. Min. Sci.* **2019**, *123*, 104094. [CrossRef]
28. Aydin, A. ISRM Suggested Method for Determination of the Schmidt Hammer Rebound Hardness: Revised Version. In *The ISRM Suggested Methods for Rock Characterization, Testing and Monitoring: 2007–2014*; Ulusay, R., Ed.; Springer: Cham, Switzerland, 2008. [CrossRef]
29. Sousa, L.M.O.; Gonçalves, B.M.M. Differences in the quality of polishing between sound and weathered granites. *Environ. Earth. Sci.* **2013**, *69*, 1347–1359. [CrossRef]

30. Kompaníková, Z.; Gomez-Heras, M.; Michňová, J.; Durmeková, T.; Vlčko, J. Sandstone alterations triggered by fire-related temperatures. *Environ. Earth Sci.* **2014**, *72*, 2569–2581. [CrossRef]
31. Sharma, P.K.; Singh, T.N. A correlation between P-wave velocity, impact strength index, slake durability index and uniaxial compressive strength. *Bull. Eng. Geol. Env.* **2008**, *67*, 17–22. [CrossRef]
32. Khandelwal, M.; Ranjith, P.G. Correlating index properties of rocks with P-wave measurements. *J. Appl. Geophys.* **2010**, *71*, 1–5. [CrossRef]
33. Ozdemir, E. A New Predictive Model for Uniaxial Compressive Strength of Rock Using Machine Learning Method: Artificial Intelligence-Based Age-Layered Population Structure Genetic Programming (ALPS-GP). *Arab. J. Sci. Eng.* **2022**, *47*, 629–639. [CrossRef]
34. ISRM. Suggested method for determining point load strength. *Int. J. Rock Mech. Min. Sci. Geomech. Abstr.* **1985**, *22*, 51–60. [CrossRef]
35. Jamshidi, A.A. Comparative Study of Point Load Index Test Procedures in Predicting the Uniaxial Compressive Strength of Sandstones. *Rock Mech. Rock Eng.* **2022**, *55*, 4507–4516. [CrossRef]
36. Garrido, M.E.; Petnga, F.B.; Martínez-Ibáñez, V.; Serón, J.B.; Hidalgo-Signes, C.; Tomás, R. Predicting the Uniaxial Compressive Strength of a Limestone Exposed to High Temperatures by Point Load and Leeb Rebound Hardness Testing. *Rock Mech. Rock Eng.* **2022**, *55*, 1–17. [CrossRef]
37. Yavuz, H.; Demirdag, S.; Caran, S. Thermal effect on the physical properties of carbonate rocks. *Int. J. Rock Mech. Min. Sci. Geomech. Abstr.* **2010**, *47*, 94–103. [CrossRef]
38. Wang, S.R.; Hagan, P.; Li, Y.C.; Zhang, C.G.; Liu, X.L. Experimental study on deformation and strength characteristics of sandstone with different water contents. *J. Eng. Sci. Tech. Rev.* **2017**, *10*, 199–203. [CrossRef]
39. Ferrero, A.M.; Marini, P. Experimental studies on the mechanical behaviour of two thermal cracked marbles. *Rock Mech. Rock Eng.* **2001**, *34*, 57–66. [CrossRef]
40. Malaga-Starzec, K.; Åkesson, U.; Lindqvist, J.E.; Schouenborg, B. Microscopic and macroscopic characterization of the porosity of marble as a function of temperature and impregnation. *Constr. Build. Mater.* **2006**, *20*, 939–947. [CrossRef]
41. Zhang, L.; Mao, X.; Lu, A. Experimental study on the mechanical properties of rocks at high temperature. *Sci. China Ser. E Tech. Sci.* **2009**, *52*, 641–646. [CrossRef]
42. Zhang, W.; Qian, H.; Sun, Q.; Chen, Y. Experimental study of the effect of high temperature on primary wave velocity and microstructure of limestone. *Environ. Earth Sci.* **2015**, *74*, 5739–5748. [CrossRef]
43. Garrido, M.E.; Martínez-Ibáñez, V.; Hidalgo-Signes, C.; Company, J.; Tomás, R. Temperature threshold of sedimentary rocks: A comparative study. In Proceedings of the ISRM International Symposium Eurock 2020—Hard Rock Engineering Trondheim, Trondheim, Norway, 14–19 June 2020.
44. Gomez-Heras, M. *Procesos y Formas de Deterioro Térmico en Piedra Natural del Patrimonio Arquitectónico*; Editorial Complutense: Madrid, Spain, 2006.
45. Tondon, S.; Gupta, V. Estimation of strength from Schmidt hammer rebound, point load index and compressional wave velocity. *Bull. Eng. Geol. Environ.* **2014**, *74*, 521–533. [CrossRef]
46. Wang, M.; Wan, W.; Zhao, Y. Prediction of the uniaxial compressive strength of rocks from simple index tests using a random forest predictive model. *Comptes Rendus Mécanique* **2020**, *384*, 3–32. [CrossRef]
47. Sadeghi, E.; Nikudel, M.R.; Khamehchiyan, M.; Kavussi, A. Estimation of unconfined compressive strength (UCS) of carbonate rocks by index mechanical tests and specimen size properties: Central Alborz zone of Iran. *Rock Mech. Rock Eng.* **2022**, *55*, 125–145. [CrossRef]
48. Elhakim, A.F. The use of point load test for Dubai weak calcareous sandstones. *J Rock Mech. Geotech. Eng.* **2015**, *7*, 452–457. [CrossRef]
49. Gomez-Heras, M.; McCabe, S.; Smith, B.J.; Fort, R. Impacts of fire on stone-built heritage. *J. Archit. Conserv.* **2009**, *15*, 47–48. [CrossRef]
50. Ozguven, A.; Ozcelik, Y. Investigation of some property changes of natural building stones exposed to fire and high heat. *Constr. Build. Mater.* **2013**, *38*, 813–821. [CrossRef]
51. Vázquez, P.; Acuña, M.; Benavente, D.; Gibeaux, S.; Navarro, I.; Gomez-Heras, M. Evolution of surface properties of ornamental granitoids exposed to high temperatures. *Constr. Build. Mater.* **2016**, *104*, 263–275. [CrossRef]